F-6-06
Extended Abstracts of the 2020 International Conference on Solid State Devices and Materials, VIRTUAL conference, 2020, pp381-382

Impact of thickness on electrical properties of SILAR-prepared BiOI photovoltaic cell studied by I-V measurement and electrochemical impedance spectroscopy analysis

R.MD Matiur [1], A.A. Abuelwafa[1], M.A.A Noman[1], S. Kato [1], N. Kishi[1] and T. Soga[1]

[1] Nagoya Institute of Technology.
Gokiso-cho, Showa-ku, Nagoya 466-8555, Japan
Phone: +81-080-4303-1166 E-mail: md.matiurrahman20@gmail.com

Abstract

This study describes the thickness effect on electrical properties and electrical impedance spectroscopy (EIS) analysis of SILAR-prepared BiOI photovoltaic cell. Moreover, the thickness of the BiOI films has increased with the increasing of the successive ionic layer adsorption and reaction (SILAR) cycle. With the change of thickness structural changes has been confirmed by sample color, Raman, XRD and SEM respectively. Here, electrical properties and EIS analysis have been discussed. Our data justify 30 is optimal SILAR cycle because it is showing maximum current density, efficiency, mobility and diffusion coefficient.

1. Introduction

As days goes the current research world getting a decent interest in the nanostructure-based inorganic thin films for the development of photovoltaic devices [1]. On the other hand, the researcher putting an effort to find the new materials for low-cost thin film-based solar cells. According to the requirement BiOI came as very attractive material for the researcher because it is safe, less toxic, and stable. It has promising optical property as well. However, to upgrade its poor electrical properties further, more research work is needed [1]. Meanwhile, with the increase of film morphology and uniformity, it is possible to improve the electrical properties. Aiming to improve, the performance analysis of various parameters is still going on.

In our study thickness of the BiOI thin film has been changed to observe the different characteristics changes.
In this paperwork, we have prepared BiOI thin film based solar cell and the cycle number for SILAR has been optimized for the cell. Moreover, characterization has done by a solar simulator, X-ray diffraction (XRD and electrochemical impedance spectroscopy (EIS).

2. Experimental process and Characterization

To analyse the electrical properties, EIS structure and morphology, BiOI was deposited on the top FTO and glass by the SILAR process. To complete one SILAR cycle, FTO or glass initially was dipped into 6mM solution of Bi $(NO_3)_3.5H_2O$ and KI respectively then once cleaned with deionized water. By this way we prepared samples for 10cycle, 20cycle, 30cycle and 35cycle. After that annealed at 100^0C for 1hour. Here, Structural characterization, morphology, optical properties and film thickness measurement were performed by XRD system (Rigaku Smartlab XRD), scanning electron microscopy (SEM, JSM-6510) and double beam spectrophotometer (JASCO V-570) and film thickness measured by Dektak 150 Surface profiler Measurement (Dektak 150) respectively. Again, to get the photo-current-voltage (I-V) and dark current measurement, a solar simulator (100 mW.cm^{-2}, AM 1.5 illumination) with the area of 0.16 cm^2 covered by a square still mask has been used.

3. Result and discussions

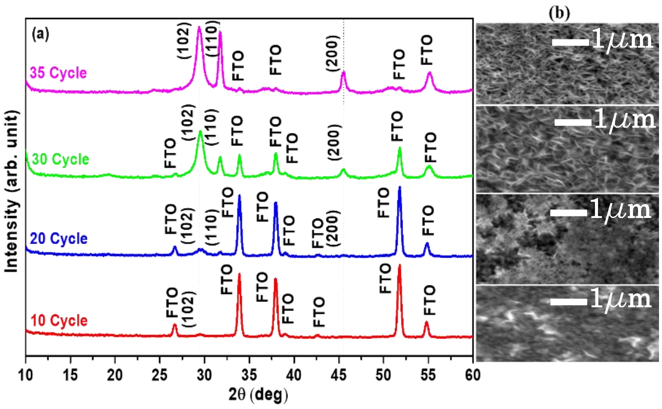

Fig. 1 (a) XRD pattern and (b) SEM view of the sample under cycle conditions for the BiOI/FTO thin films

The XRD analysis confirms the plane (102), (110), and (200) exist in 2θ at, 29.7°, 31.7°, and 45.5° with different intensities which have shown in Fig.1(a). Again, it showed that the growth of (200) and (110) planes happen with higher intensity after 30 cycle and 20 cycle respectively. Whereas the intensity of the (102) plane and crystallite size (7.64nm to 10.19nm) increases with cycle number. With the increase of SILAR cycle optical band gap decreases from 1.97eV to 1.84eV and thickness increased from 80nm to 625nm. On the other hand, from the SEM view in Fig. 1(b) it has been confirmed that with increase of cycle flakes density also increases. Solar cell charge transport, transfer and accumulation methods can be calculated by using the EIS spectrum analysis which known as a Nyquist plot [2]. Here, Fig. 2 shows the Nyquist plot of BiOI cell prepared under different SILAR cycle condition and we found single semicycle for every SILAR cycle. Moreover, equivalent circuit also included in Fig. 2. This Nyquist plot helps to calculate equivalent circuit series resistance, R_s and parallel resistance, R_p which showed in

Table I Device parameters of BiOI cell under different cycle number

Cycle number	Jsc (mA/cm^2)	Voc (V)	FF	Efficiency (%)	R_S kΩ	R_p MΩ	τ_d (ns)	D (cm^2/s)	μ ($cm^2V^{-1}S^{-1}$)
10	0.37	0.41	0.471	0.071	2.28	1.49	485.74	0.0001	0.0051
20	0.43	0.43	0.465	0.085	1.62	0.62	360.33	0.0014	0.0544
30	0.60	0.43	0.428	0.109	1.50	0.36	359.93	0.0108	0.4182
35	0.16	0.32	0.326	0.017	3.08	0.55	360.57	0.0068	0.2638

Table I. R_p has an impact on the recombination resistance, R_{ac}. Here, minimum R_s and R_p has been observed for 30 SILAR cycle. Again, by using the bode plot in we have calculated the frequency f_{max} and capacitance, Cp. Again, with the help of R_p and C_p it is possible to describe the recombination process such as diffusion time (τ_d), recombination resistance, diffusion coefficient (D), mobility (μ) of the BiOI/FTO glass substrate based solar cell [3]. In our study 30cycle is the optimum cycle number for SILAR process because it is showing the lower diffusion time, faster transportation process and maximum mobility. As it is showing maximum diffusion coefficient and mobility therefore, we will get maximum electrical properties also [2] which has confirmed by I-V measurement.

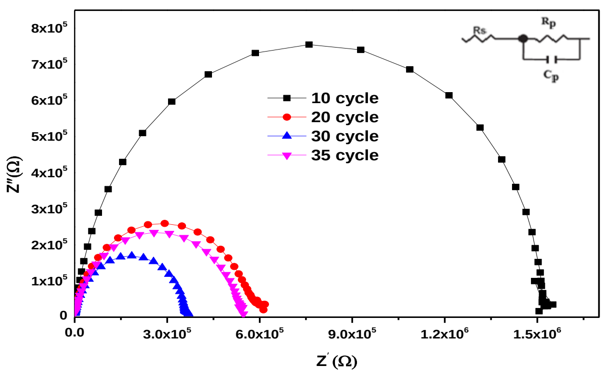

Fig.2 Nyquist plot of the BiOI cells prepared under different SILAR cycle condition

The dielectric constant ε_1, ε_2 and electrical modulus M' ,M''have been calculated by using the reported equation [3]. Here, ε_1, ε_2 presented with respect to frequency in Fig.3(a) which gives us the idea about the capacitive nature and dielectric losses of the cell. On the other hand, graphical view in Fig. 3(b) of M' and M'' with respect to frequency represents the mechanism of the electrical transport, carrier hopping, relaxation and conductivity relaxation process. At lower frequency both ε_1 and ε_2 are maximum which indicates at the interface region of sample and electrode, charge generation is higher and dielectric loss or required energy for molecular motion respectively. Moreover, at higher frequency $\varepsilon_1$tends to zero that means no time for charge generation. On the other hand, at lower frequency M' and M'' tend to zero that gives the information about no electrode polarization phenomenon and constant increase tell us about short range mobility of the carrier. At higher frequency M'' showing the behavior of the non-Debeye type [3]. With the increase of frequency shifting of the peak at right side indicate the better electrical transport and conductivity relaxation process. At 35 cycle flakes number increases highly which causes reduction of film uniformity and large number of charge collusion because of high density flakes. There are some isolation areas have generated for higher density of flakes at 35 cycle which confirmed from SEM view. These isolated areas are causing the electron trapping. As a result of that we got poor electrical properties for 35 SILAR cycle.

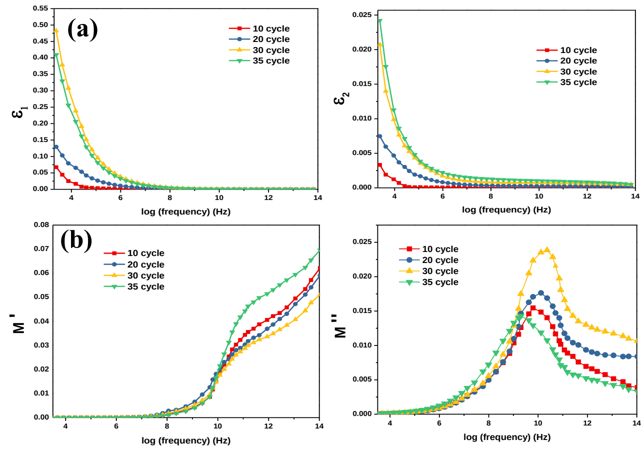

Fig.3 (a) ε_1, ε_2VS log (frequency) (b) M', M''VS log (frequency)

4. Conclusion:

EIS analysis for the SILAR-prepared BiOI/FTO cell has been done for the first time. In our study optimal cycle number for the SILAR process is 30 because it is showing the minimum diffusion time 359.6ns, maximum diffusion coefficient (D) 0.01 cm^2/s, maximum mobility(μ) 0.42 $cm^2V^{-1}S^{-1}$. Moreover, from the electrical properties maximum current density (J_{sc}) 0.6 mA/cm^2, maximum efficiency 0.109% have been observed for the 30cycle as well.

References

[1] A. A. Putri, S. Kato, N. Kishi, and T. Soga, J. Sci. Adv. Mater. Devices, no. vol 4, pp. 116–124, 2019.

[2] H. C. Sun, Y. H. Luo, Y. D. Zhang, D. M. Li, Z. X. Yu, K. X. Li, and Q.B. Meng, J. Phys. Chem. C, vol. 114, pp. 11673–11679, 2010.

[3] A. A. Abuelwafa, M. D. M. M. El, and N. T. Soga, *Appl. Phys. A*, no. vol. 124, pp. 266, 2018.